

# PV FED DC-DC Converter With Two Input Boost Stages

M.Arunkumar, Mr.K.Palanivelrajan

**Abstract**— Renewable energy system is getting a importance in the energy generation due to their clean and environment features .The renewable systems usually generate a lower voltage which requires a high step up dc-dc converter at the front end .In order to meet the requirements of the grid the low voltage has to stepped up, which a basic boost converter cannot be employed due to its high duty ratio requirements which leads a high switch loss that degrades the efficiency. In order to alleviate the issues related to the high gain conversion with bigger efficiency a new converter based on the isolated resonant topology is introduced which can be used to draw power from renewable sources with a minimal loss. The isolated resonant functionality enables the converter to operate high gain and maximum efficiency by introducing the zero-voltage switching and zero-current switching for all of the active switches and the diodes respectively in operating range which makes the converter suitable for renewable application. The effectiveness of the proposed method is carried out and the results are presented and it shows that converters operates high gain ratio with an efficiency of 97.2%.

**Index Terms**— Boost Converter, isolated Resonant Converter, zero-voltage switching and zero-current switching

## I. INTRODUCTION

Renewable sources are one of the significant players in the world's energy portfolio, and it will make one of the biggest contributions to electricity generation. The dc/dc converters are employed in PV systems.

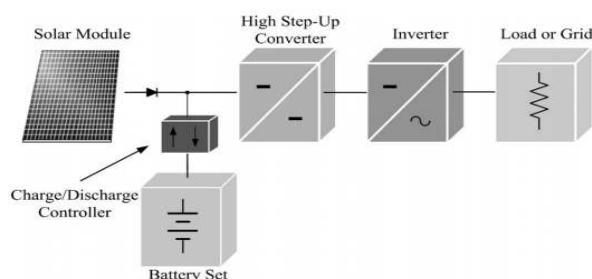


Fig 1.1typical renewable energy conversion system PV based Converter topologies

In order to meet the grid requirements a converter with a high step up gain ratio and the high efficiency are more important. High voltage conversion ratios is obtained by dc-dc power electronic converters . An interleaved boost converter is applicable for high step-up and high-power application. The

**Arunkumar M** was born on November 16, 1993. He received his B.E. degree in Electrical and Electronics Engineering in 2015 in M.Kumarasamy College of Engineering, Karur, Tamil Nadu, India

**Palanivel Rajan K**, Assistant Professor in the department of Electrical and Electronics Engineering at PSNA College of Engineering and technology, Dindigul, Tamil Nadu

high step-up interleaved converter with a voltage multiplier module is composed of coupled inductors and capacitors and is inserted between a conventional interleaved boost converter. The interleaved boost converter one switch is ON condition at the time other switch is OFF condition alternatively switches to act in the converter. This converter can be used to draw power from two independent dc sources as a multiport converter. They draw continuous input current from both the input sources with low current ripple which is required in many applications, e.g., solar. Voltage is boosted up by diode-capacitor voltage multiplier stages. Voltage multiplier stages to limit the voltage stresses on the switches, diodes and capacitors. Also Losses factor and efficiency are proposed in isolated resonant converter.

## II. NON-ISOLATED STEP UP CONVERTER

The high step-up interleaved converter have two diodes and two switched capacitors. When the switches turn off , the phase whose switch is in OFF state performs as a fly back converter, and the other phase whose switch is in ON state performs as a forward converter.

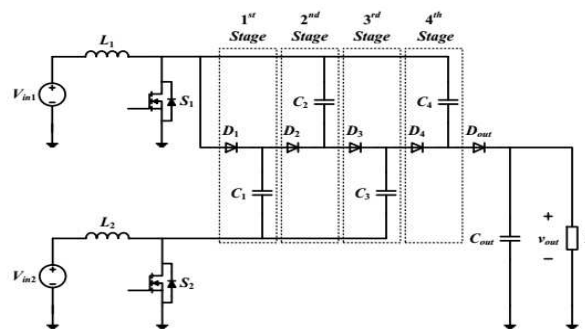


Fig 2.1 Topology design of the high step up converter

### A) Modes of Operation:

For normal operation of the converter, overlapping time exists when the switching states are transient at any given time. Therefore, the converter has modes of operation as follows. The converter can operate when the switch duty ratios are small and there is no overlap time between the conduction of the switches.

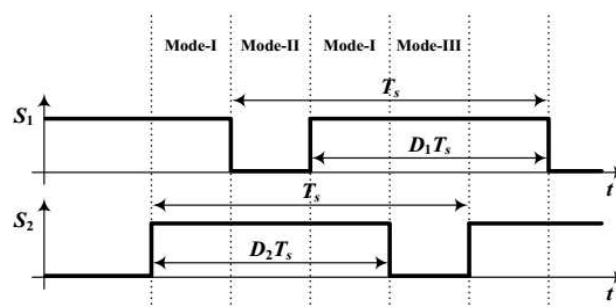


Fig 2.2 switching strategy of the converter

In this mode both switches S1 and S2 are ON. Both the inductors are charged from their input sources  $V_{in1}$  and  $V_{in2}$ . The current in both the inductors rise linearly. The reverse biased diodes do not conduct in different VM stages. In VM stages the load is supplied by the output capacitor  $C_{out}$ .

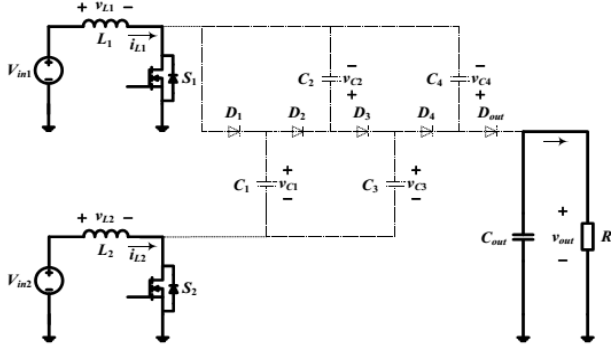


Fig2.3 Mode I of operation for the converter

In this mode switch S1 is OFF and S2 is ON. Diodes are numbered by odd and even numbers. The odd numbered diodes are forward biased and even numbered diodes are reverse biased. Odd numbered VM stages, the load is supplied by output capacitor alone. However, even numbered VM stages, the load is supplied by output capacitor which is charged by diode. The load is supplied by capacitor and diode in case of four VM Stages.

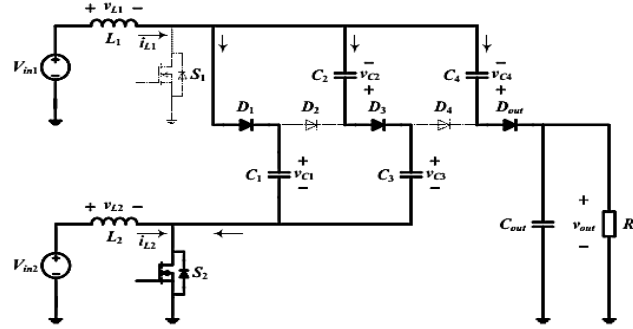


Fig. 2.4 Mode II of operation for the converter

In this mode switch S1 is ON and S2 is OFF. In this mode even numbered diodes are forward biased and charging. The odd numbered capacitors are discharging. If VM stages are odd numbered, then the output diode  $D_{out}$  is charging the output capacitor and supply the load.

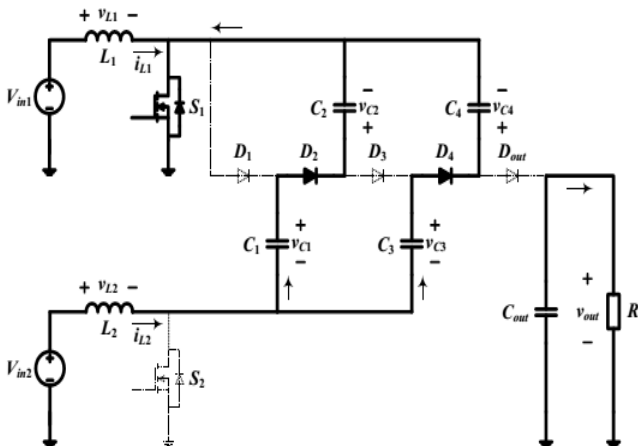


Fig2.5 Mode III of operation for the converter

In the even numbered VM stages, the capacitor alone supplies the load. For a converter with four stages of VM for the voltage gain. For L1 one can write

$$V_{L1} = 0 \quad (1)$$

Therefore above fig can be observed that the capacitor voltages can be written in terms of upper boost switching node voltage as

$$V_{C1} = V_{C3} - V_{C2} = V_{out} - V_{C4} = \frac{V_{in1}}{(1-d_1)} \quad (2)$$

where  $d_1$  is the switching duty cycle for S1. Similarly, from the volt-sec balance of the lower leg boost inductor L2, one can write the capacitor voltages in terms of lower boost switching node voltage as

$$V_{C2} - V_{C1} = V_{C4} - V_{C3} = \frac{V_{in2}}{(1-d_2)} \quad (3)$$

where  $d_2$  is the switching duty cycle for S2.

From (2) and (3), the capacitor voltages can be derived as

$$\begin{aligned} V_{C1} &= \frac{V_{in1}}{(1-d_1)} \\ V_{C2} &= \frac{V_{in1}}{(1-d_1)} + \frac{V_{in2}}{(1-d_2)} \\ V_{C3} &= \frac{2V_{in1}}{(1-d_1)} + \frac{V_{in2}}{(1-d_2)} \\ V_{C4} &= \frac{V_{in1}}{(1-d_1)} + \frac{2V_{in2}}{(1-d_2)} \end{aligned} \quad (4)$$

from (2) output voltage is derived, which is given by

$$\begin{aligned} V_{out} &= V_{C4} + \frac{V_{in1}}{(1-d_1)} \\ &= \frac{3V_{in1}}{(1-d_1)} + \frac{2V_{in2}}{(1-d_2)} \end{aligned} \quad (5)$$

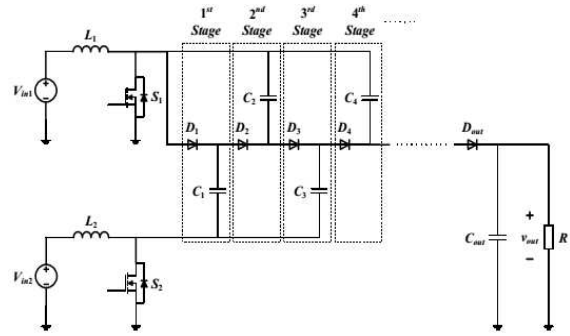


Fig. 2.6 converter with N number of VM stages.

Similar analysis can be achieved N number of VM stages. Hence the VM stage capacitor voltages are given by

$$\begin{aligned} V_{cn} &= \left(\frac{n+1}{2}\right) \frac{V_{in1}}{(1-d_1)} + \left(\frac{n-1}{2}\right) \frac{V_{in2}}{(1-d_2)} \text{ if } n \text{ is odd \& } n \leq N \\ V_{cn} &= \left(\frac{n}{2}\right) \frac{V_{in1}}{(1-d_1)} + \left(\frac{n}{2}\right) \frac{V_{in2}}{(1-d_2)} \text{ if } n \text{ is even \& } n \leq N \end{aligned} \quad (6)$$

The output voltage equation depends on whether N is odd or even and is given by

$$\begin{aligned} V_{out} &= V_{CN} + \frac{V_{in2}}{(1-d_2)} \text{ if } N \text{ is odd} \\ &= \left(\frac{N+1}{2}\right) \frac{V_{in1}}{(1-d_1)} + \left(\frac{N+1}{2}\right) \frac{V_{in2}}{(1-d_2)} \end{aligned} \quad (7)$$

$$\begin{aligned} V_{out} &= V_{CN} + \frac{V_{in1}}{(1-d_1)} \text{ if } N \text{ is even} \\ &= \left(\frac{N+2}{2}\right) \frac{V_{in1}}{(1-d_1)} + \left(\frac{N}{2}\right) \frac{V_{in2}}{(1-d_2)} \end{aligned} \quad (8)$$

When the converter operates in an interleaved manner with single input source, if  $d_1$  and  $d_2$  are also chosen to be identical, i.e.,  $d_1 = d_2 = d$ , then the output voltage is obtained as

$$V_{out} = (N+1) \frac{V_{in}}{(1-d)} \quad (9)$$

The output voltage equation for alternative VM stages is given by

$$V_{out} = \left(\frac{N+1}{2}\right) \frac{V_{in1}}{(1-d_1)} + \left(\frac{N+1}{2}\right) \frac{V_{in2}}{(1-d_2)} \quad \text{if } N \text{ is odd} \quad (10)$$

In order to verify the performance of the converter a model with a steady state control has been developed with four VM stages and with interleaved boost input stage with a single source was built to verify the operation. The VM stage capacitors are selected such that the equivalent series resistance due to charging/discharging of the capacitors is low keeping the total capacitance to reasonable levels, thus improving the efficiency and output voltage regulation.

### III. ISOLATED STEP UP AND STEP DOWN CONVERTER

Isolated dc-dc converters are being preferred due to their galvanic isolation capabilities between the source and the load sides, the efficiency is greatly depend up on it, without transformers the isolation part is cannot be determined. Resonant converters have become increasingly popular due to their higher harmonic voltages are filtered by the resonant network, a nearly sinusoidal current appears at the input of the resonant, which enables zero voltage switching or zero current switching of switching devices. Sacrificing the efficiency at the maximum or minimum input voltage which makes the utilization of the such resonant converters for a high stepup conversions. The topologies of the conventional RVMR, where  $C_{r1}$  and  $C_{r2}$  are resonant capacitors,  $L_r$  is a resonant inductor,  $D_1$  and  $D_4$  are output diodes,  $D_2$  and  $D_3$  are regenerative diodes, T is a high frequency transformer, and  $S_1$  and  $S_2$  are the active switches through which the output power can be regulated. Referenced to the output ground.

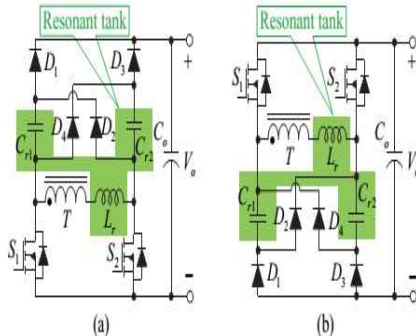


Fig 3.1: Conventional resonant voltage multiplier rectifiers  
(a) N-Type, (b) P-Type

The resonant tank is composed of three elements,  $C_{r1}$ ,  $C_{r2}$  and  $L_r$ . In the N-Type RVMR, the two switches  $S_1$  and  $S_2$  are placed on the underside of the rectifier and connected to the negative potential of the output voltage  $V_o$ , while in the P-Type RVMR, the two switches are connected to the positive potential of the  $V_o$ . Different from traditional RC topologies that using variable frequency control to regulate output power, the resonant tank in the RVMR always operates at the resonant frequency.

$$f_r = \frac{\omega_r}{2\pi} = \frac{1}{2\pi \sqrt{L_r(C_{r1} + C_{r2})}} \quad (11)$$

When the switches in the RVMR are ON, the voltage on the secondary-winding of the transformer is directly applied on the resonant inductor, in which case, the inductor acts as a

boost inductor in resonant condition. Therefore, for good operation of the RVMR, the transformer T should be able to generate high frequency voltage, which is a basic requirement of the RVMR. The main focus of existing approach is the RVMR. The full-bridge RC is taken as an example and to be analyzed to explain the control and operation principles.  $L_m$  doesn't participate in the resonant or the power transferring of the converter, but it can help to realize soft-switching of the primary side switches. In practice, the leakage inductance of the transformer T is used as a part of the resonant inductance  $L_r$ . The average voltage across  $C_{r1}$  and  $C_{r2}$  is only half of the output voltage. For simplicity, normalized voltage gain G is defined as

$$G = \frac{V_o}{2n V_{in}} \quad (12)$$

All switches operate at the resonant frequency determined by (11). Phase-shift control strategy is employed to control the output voltage and power. The primary-side phase-shift angle,  $\phi_P$ , is defined to be the phase difference between the gate signals of  $S_1$  and  $S_4$ , while the secondary-side phase-shift angle,  $\phi_S$ , is defined to be the phase difference between the gate signals of  $S_4$  and  $S_6$ . For simplicity, equivalent primary-side and secondary-side phase-shift duty cycles  $d_{\phi P}$  and  $d_{\phi S}$  are defined:

$$d_{\phi P} = \frac{\phi_P}{\pi}, \quad d_{\phi S} = \frac{\phi_S}{\pi}.$$

When the voltage conversion ratio  $G \geq 1$ , the converter operates in the boost mode, in which, the primary-side duty cycle  $d_{\phi P}$  is constant  $d_{\phi P} = 1$ , and the secondary-side duty cycle  $d_{\phi S}$  controls the voltage and power of the output. The steady state of the resonant inductor current,  $i_{Lr}$ , and resonant capacitor voltage,  $v_{Cr1}$  for easily understanding the operation of the converter. the inductor current is analysed by multiplying the impedance of the resonant tank,  $Z_r$ .

$$Z_r = \sqrt{\frac{L_r}{C_{r1} + C_{r2}}} = \sqrt{\frac{L_r}{2C_r}} \quad (13)$$

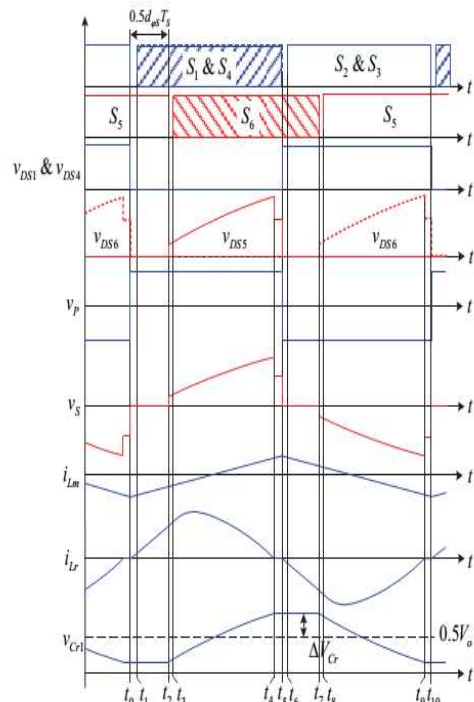


Fig 3.2: Key waveforms of the RC in the boost mode



In Stage 1  $[t_0, t_1]$ , before  $t_0$ , the switches  $S_2$ ,  $S_4$  and  $S_5$  are ON,  $i_{Lr}$  has been reset to zero. At  $t_0$ ,  $S_2$  and  $S_4$  turn OFF, entering a period of dead time. The magnetizing inductor  $L_m$  acts as a current source during this short time period to discharge the drain-source voltages of the switches  $S_1$  and  $S_4$ , resulting in ZVS of  $S_2$  and  $S_4$ . Meanwhile, the input voltage is directly applied on the resonant inductor  $L_r$ . So the inductor current increases linearly.

$$i_{Lr}(t) = \frac{nV_{in}}{L_r}(t - t_0) \quad (14)$$

In Stage 2  $[t_1, t_2]$ , at  $t_1$ ,  $S_1$  and  $S_4$  turn ON with ZVS. The equivalent circuit of the resonant inductor in the Stage 1 and Stage 2, where the operation of the proposed RC is similar to a conventional PWM boost converter. Stage 4  $[t_2, t_4]$ , at  $t_2$ ,  $S_5$  turns OFF. The current of  $L_r$  has been charged to an initial condition and now the converter operates similar to a series-resonant converter.  $L_r$  and the parallel combination of  $C_{r1}$  and  $C_{r2}$  begin to resonate. In this stage, the diodes  $D_2$ ,  $D_4$  and the body diode of  $S_6$  are ON. Stage 4  $[t_4, t_5]$ , at  $t_4$ ,  $S_6$  is turned on with ZVS. During Stage 4 and Stage 4, the capacitor  $C_{r1}$  is charged while  $C_{r2}$  is discharged. The equivalent circuit of the resonant tank of these two stages. The capacitor voltage always satisfies  $V_{Cr1} = V_o - V_{Cr2}$ , so the average voltage of the two capacitors are the same and satisfy  $V_{Cr1} = V_{Cr2} = 0.5V_o$ . The resonant stage ends when the current  $i_{Lr}$  reaches zero and the diodes  $D_2$  and  $D_4$  turn

OFF with zero-current and without reverse-recovery losses. Stage 5  $[t_4, t_5]$  at  $t_4$ ,  $i_{Lr}$  reaches zero, the converter enters an idle stage in which no power is being transferred to the load. From  $t_5$ , the other half switching cycle begins.

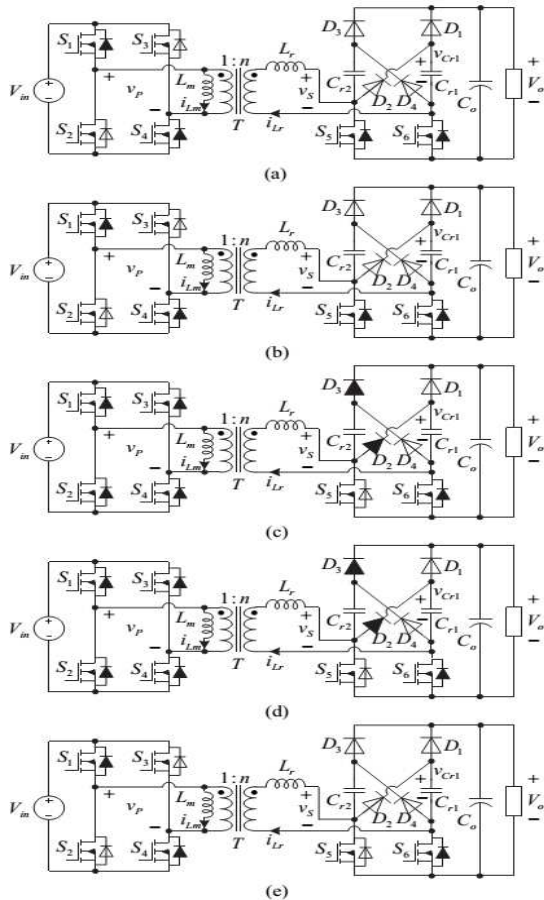


Fig 3.3: Boost mode Equivalent circuits in different stages, (a)  $[t_0, t_1]$ , (b)  $[t_1, t_2]$ , (c)  $[t_2, t_4]$ , (d)  $[t_4, t_4]$  and (e)  $[t_4, t_5]$

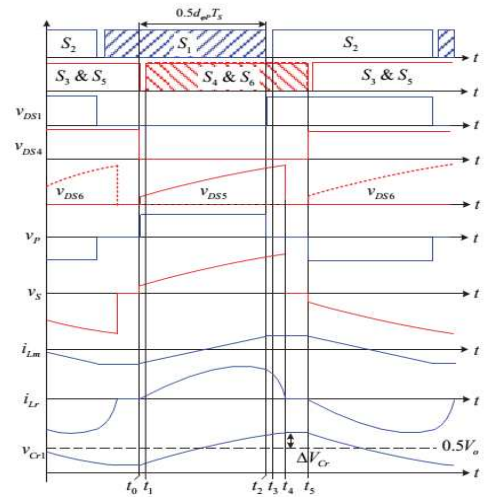


Fig 3.4: Key waveforms of the RC in the buck mode

In Stage 1  $[t_0, t_1]$ : Before  $t_0$ ,  $S_1$ ,  $S_4$  and  $S_5$  are ON,  $i_{Lr}$  has resonated to zero. At  $t_0$ ,  $S_4$  and  $S_5$  turn OFF.  $L_m$  acts as a current source to discharge the drain-source voltage of  $S_4$ . So  $S_4$  can be turned ON under ZVS condition. Meanwhile,  $L_r$  and the parallel combination of  $C_{r1}$  and  $C_{r2}$  begin to resonate. The diodes  $D_2$ ,  $D_4$  and the body diode of  $S_6$  are ON. Stage 2  $[t_1, t_2]$  At  $t_1$ , switches  $S_4$  and  $S_6$  turn ON with ZVS. During Stage 1 and Stage 2, the converter operates similar to a conventional series resonant converter. The equivalent circuit of the resonant tank.  $L_r$  and the parallel combination of  $C_{r1}$  and  $C_{r2}$  resonate as the converter moves. capacitor  $C_{r1}$  is charged by  $L_r$  while capacitor  $C_{r2}$  is discharged.

$$i_{Lr}(t) = \frac{r}{Z_r} \sin[\omega_r(t - t_0)] \quad (15)$$

$$V_{Cr1}(t) = nV_{in} - r \cos[\omega_r(t - t_0)] \quad (16)$$

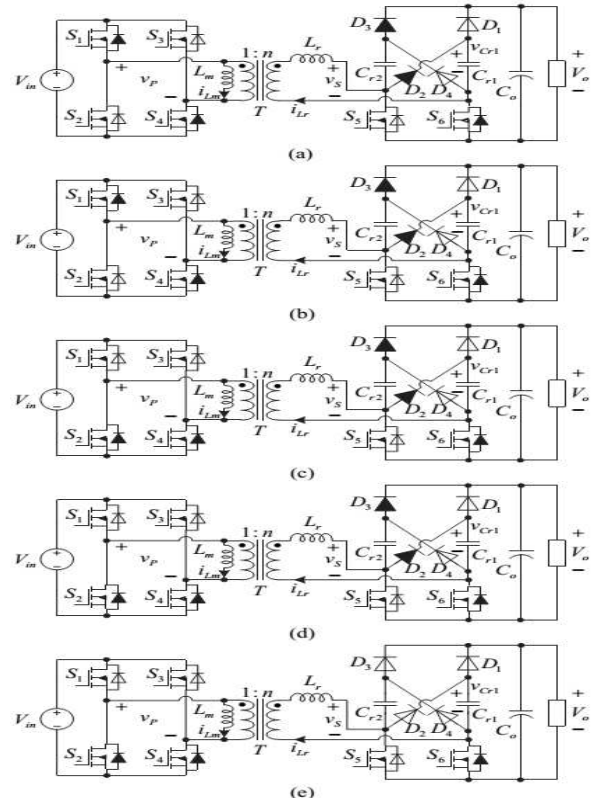


Fig 3.5: Buck mode Equivalent circuits in different stages, (a)  $[t_0, t_1]$ , (b)  $[t_1, t_2]$ , (c)  $[t_2, t_4]$ , (d)  $[t_4, t_4]$  and (e)  $[t_4, t_5]$

In Stage 4  $[t_2, t_4]$  at  $t_2$ ,  $S_1$  is OFF. The drain-source voltage of  $S_2$  is discharged by the magnetizing and resonant currents. So  $S_2$  can be turned ON with ZVS. Stage 4  $[t_4, t_4]$ , at  $t_4$ ,  $S_2$  turns ON with ZVS. During Stage 4 and Stage 4,  $C_{r1}$ ,  $C_{r2}$  and  $L_r$  resonate. This stage ends when the current of  $L_r$  reaches zero and the rectifier diodes turn OFF with zero-current and without reverse-recovery losses. Stage 5  $[t_4, t_5]$ , at  $t_4$ ,  $i_{Lr}$  reaches zero, the converter enters an idle stage. No power is being transferred to the load. From  $t_5$ , the other half switching cycle begins.

i.

Boost Mode with Secondary-Side Phase-Shift Control:

When the converter works in the boost mode with  $G \geq 1$  and secondary-side phase-shift control, according to the operation principles and waveforms, and ignoring the power losses, thus the power calculated is as follows

$$P_{in} = \frac{nV_{in} \int_0^{t_3} i_{Lr}(t) dt}{T_{s/2}} = P_0 = \frac{V_0^2}{R_0} \quad (17)$$

$$G = 1/2 \sqrt{1 + \frac{\pi d^2 \varphi^2}{2Q}} \quad (Q = \frac{Z_r}{R_0}) \quad (18)$$

ii.

Buck Mode with Primary-Side Phase-Shift Control:

When the task of converter in the buck mode with  $G \leq 1$  and primary-side phase-shift control, according to the operation principles and waveforms, thus the power calculated is as follows

$$P_{in} = \frac{nV_{in} \int_0^{t_2} i_{Lr}(t) dt}{T_{s/2}} = P_0 = \frac{V_0^2}{R_0} \quad (19)$$

$$G = \frac{-B \pm \sqrt{B^2 - 4AC}}{2A} \quad (20)$$

$$\text{(Where, } A = \frac{2\sqrt{2}}{f_r}; B = 2(\cos \pi d \varphi_p - 1) \left( \frac{1}{\sqrt{2} f_r} - \frac{1}{4\sqrt{2} f_r Q} \right); \\ C = \frac{1}{2\sqrt{2} f_r Q} (\cos \pi d \varphi_p - 1))$$

The main constraints for designing the parameters of resonant tank,  $L_r$  and  $C_r$ , are resonant frequency and output power. The relationship between the voltage ripple on the resonant capacitance and the output power has been given. The maximum voltage ripple should be lower than the DC voltage on the capacitor, which is equal to half of the output voltage. Therefore, the value of resonant capacitance should satisfy

$$C_r > \frac{P_0 T_s}{2V_0^2} \quad (21)$$

$$L_r < \frac{V_0^2}{2\omega_0^2 P_0 T_s} \quad (22)$$

Substituting  $V_0=400V$ ,  $P_0=400W$  and  $T_s=10\mu s$  into (22), we have  $C_r > 12.5nF$ . Resonant inductor  $L_r$  should satisfy the parameters into (22), then  $L_r < 101\mu H$ . Two 22nF capacitors are used as the resonant capacitors. The transformer turns ratio was selected to be  $n=4$  according to the normal voltage to make the normalized voltage gain  $G=1$  at  $V_{in}=50V$ . Then the highest efficiency can be achieved at this voltage, and the operation voltage ranges of the buck and boost modes are equal.

The conventional full-bridge LLC resonant converter is selected for performance comparison due to the similar characteristics. In the LLC resonant converter the magnetizing inductance ( $L_m$ ) has to be decreased to provide the desired voltage conversion ratio, so the circulating current

introduced by the  $L_m$  which is much larger than the proposed converter.

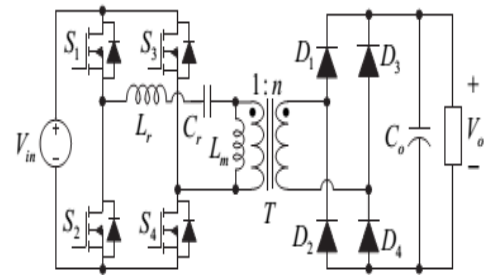


Fig 3.6: Full-bridge LLC resonant converter

However, the conduction losses of the rectifier diodes of the LLC resonant converter are lower than the proposed converter. Fortunately, the current of the secondary-side is much lower due to high output voltage, and the voltage stresses of the two upper diodes,  $D_1$  and  $D_4$ , and switches  $S_5$  and  $S_6$  in the existed converter are lower than the rectifying diodes in the LLC resonant converter. Therefore, low voltage-rated diodes and switches with lower conduction losses and better switching performance can be used to reduce the power losses. In order to verify the performance of the proposed converter a model with a model has been developed with an isolated dc-dc conversion with a secondary control stage with a single source was built to verify the operation.

#### IV. SIMULATION RESULTS

In order to validate the performance of the high step up converter along with the isolated conversion scheme with the source modeling in MATLAB /PLEXIM and the experimental waveforms are developed.

A) Non isolated step up converter

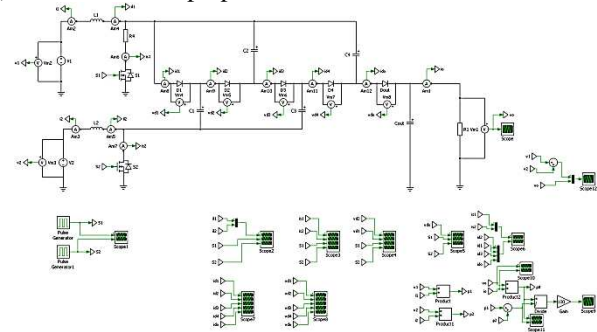


Fig 4.1 Non isolated step up converter system simulation diagram

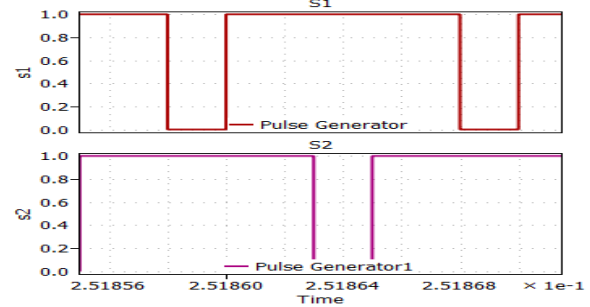


Fig 4.2 PWM for the converter with X axis in time in seconds Y axis in Voltage

From the fig.(4.2) it can be stated that the converter with the a single input source will have identical duty ratios  $d_1$  and  $d_2$ , i.e.,  $d_1 = d_2 = d$ , both the boost stages will always have symmetrical.

## PV FED DC-DC Converter With Two Input Boost Stages

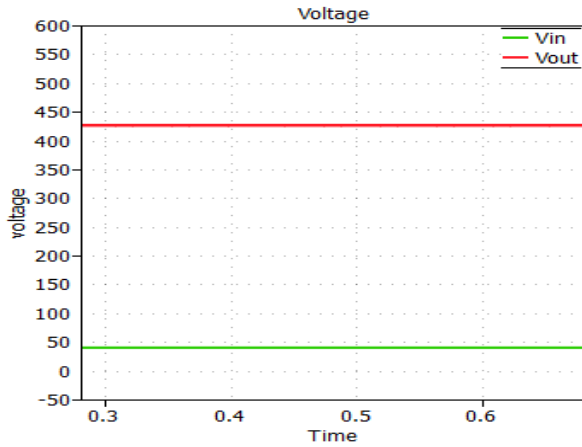


Fig 4.3 Input voltages to the converter with source A & B

Fig 4.3 The converter output voltages under the 40 V source input produces the output voltage around 420 V with Voltage in Y axis and time in X axis.

B) Isolated step up and step down converter

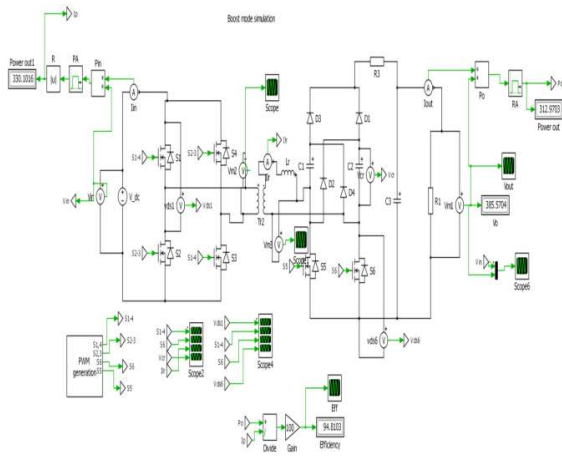


Fig 4.4 Isolated step up and step down converter simulation diagram.

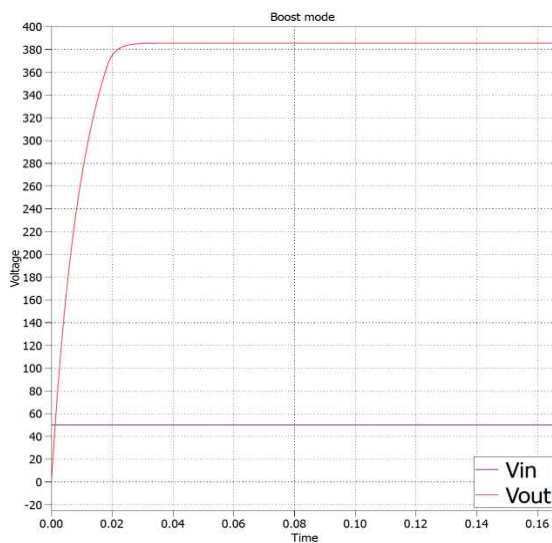


Fig. 4.5 Step up Converter output

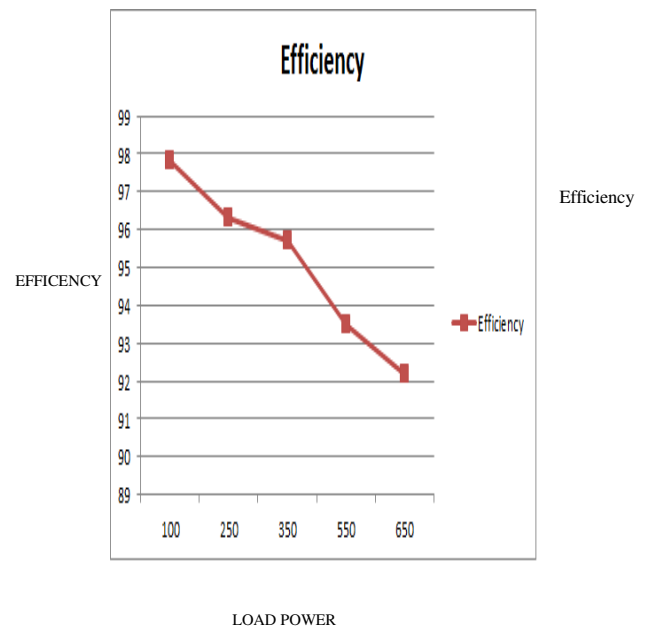


Fig 4.6 Step up Converter Load Power Vs. Efficiency

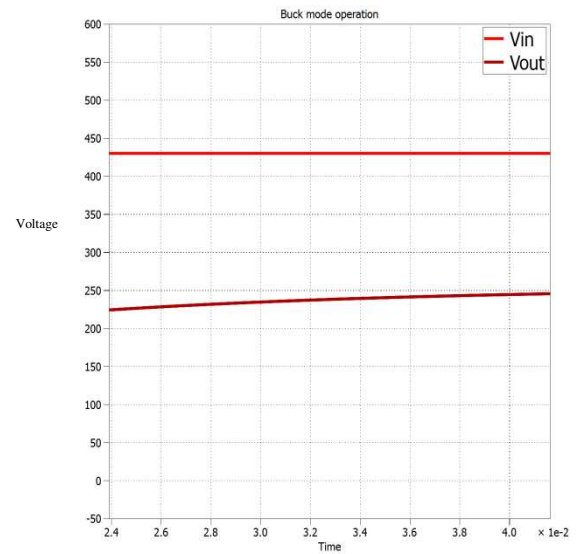


Fig 4.7 Isolated Step down Converter Output

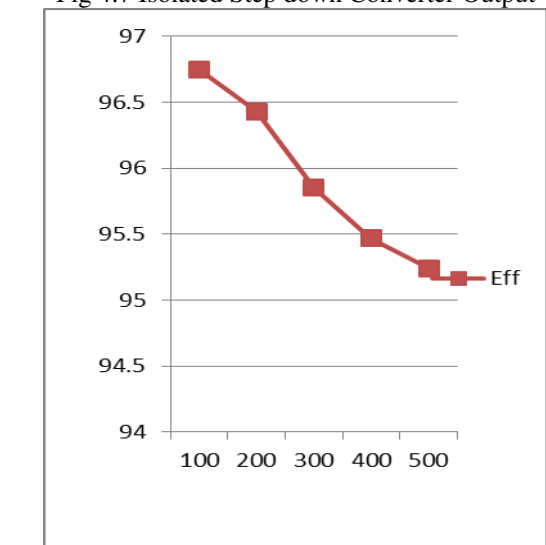


Fig 4.8 Step down Converter Load Power Vs. Efficiency

## V. CONCLUSION

A high voltage gain dc-dc converters with isolated resonant voltage multipliers are been presented and validated .The proposed converter yields a better efficiency and gain and more over the converter can realize zero-voltage switching for active switches and zero-current switching for diodes. In addition, the converter is suitable for wide voltage applications due to its isolated Buck and Boost conversion capability suitable for renewable power applications. Theoretical analysis and experimental results indicate that the proposed converter can realize soft-switching for all of the switching devices in a wide range, low circulating energy, voltage regulation and high efficiency through simple constant-frequency dual phase-shift control. The experiments with the 400W prototype have clearly demonstrated the claimed features, and indicated that the proposed converter is suitable for high efficiency isolated power conversion with wide load and voltage ranges.

## REFERENCE

- [1] Y.-P. Hsieh, J.-F.Chen, T.-J.Liang, and L.-S. Yang(2011), "A novel high step-up DC–DC converter for a microgrid system," IEEE Trans. Power Electron.,vol. 26, no. 4, pp. 1127–1136.
- [2] D. Huang, S. Ji, F. C. Lee(2014), "LLC resonant converter with matrix transformer," in Proc. IEEE APEC, pp. 1118-1125.
- [3] S. Jain and V. Agarwal(2007), "A single-stage grid connected inverter topology for solar PV systems with maximum power point tracking," IEEE Trans.Power Electron., vol. 22, no. 5, pp. 1928–1940.
- [4] Y. Jang and M. M. Jovanovic(2007), "Interleaved boost converter with intrinsic voltage-doubler characteristic for universal-line PFC front end," IEEETrans. Power Electron., vol. 22, no. 4, pp. 1394–1401.
- [5] S. Lee, P. Kim, and S. Choi(2013), "High step-up soft-switched converters using voltage multiplier cells," IEEE Trans. Power Electron., vol. 28, no. 7,pp. 3379–3387.
- [6] W. Li, Y. Zhao, Y. Deng, and X. He(2010), "Interleaved converter with voltage multiplier cell for high step-up and high-efficiency conversion," IEEETrans. Power Electron., vol. 25, no. 9, pp. 2397–2408.
- [7] C.-M. Young, M.-H.Chen, T.-A.Chang, C.-C.Ko, and K.-K. Jen(2013), "CascadeCockcroft–Walton voltage multiplier applied to transformerlesshighstep-up DC–DC converter," IEEE Trans. Ind. Electron., vol. 60, no. 2,pp. 523–537.
- [8] K.-C. Tseng, C.-C.Huang, and W.-Y. Shih( 2013), "A high step-up converter with a voltage multiplier module for a photovoltaic system," IEEE Trans.Power Electron., vol. 28, no. 6, pp. 3047–3057.



**Arunkumar M** was born on November 16, 1993. He received his B.E. degree in Electrical and Electronics Engineering in 2015 in M.Kumarasamy College of Engineering, Karur, Tamil Nadu, India and he is pursuing M.E(2<sup>nd</sup> year ) in Power Electronics and Drives, in at PSNA College of Engineering and technology, Dindigul, Tamil Nadu India.



**Palanivel Rajan K** completed his B.E in Electrical and Electronics Engineering at RVS College of Engineering, Dindigul in 2007 and M.E., degree in Applied Electronics from College of Engineering, Guindy in the year 2009. His area of interest includes Digital Systems. Currently he is working as an Assistant Professor in the department of Electrical and Electronics Engineering at PSNA College of Engineering and technology, Dindigul, Tamil Nadu.